Supporting Information

Boosting the Conversion Efficiency Over 20 % in $MAPbI_3$ Perovskite Planar Solar Cells by Employing Solution-Processed Aluminum-Doped Nickel Oxide Hole Collector

Bhaskar Parida [1)], Saemon Yoon [1)], Jun Ryu [1)], Shuzi Hayase [2)], Sang Mun Jeong [3),*], and Dong-Won Kang [1), *]

[1)] School of Energy Systems Engineering, Chung-Ang University, Seoul 06974, Republic of Korea.

[2)] Info-Powered Energy System Research Center, The University of Electro-Communications, 1-5-1 Chofugaoka, Chofu, Tokyo, 182-8585, Japan

[3)] Department of Chemical Engineering, Chungbuk National University, Cheongju 28644, Republic of Korea

Corresponding Author
*E-mail: kangdwn@cau.ac.kr
*E-mail: smjeong@chungbuk.ac.kr

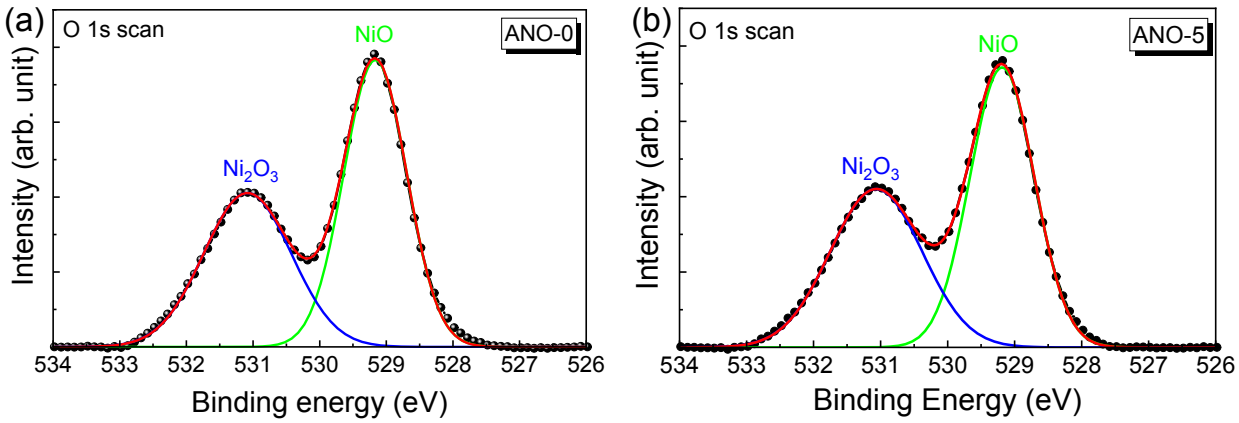

Figure S1 Deconvolution of O 1s XPS spectra of (a) ANO-0 and (b) ANO-5 films.

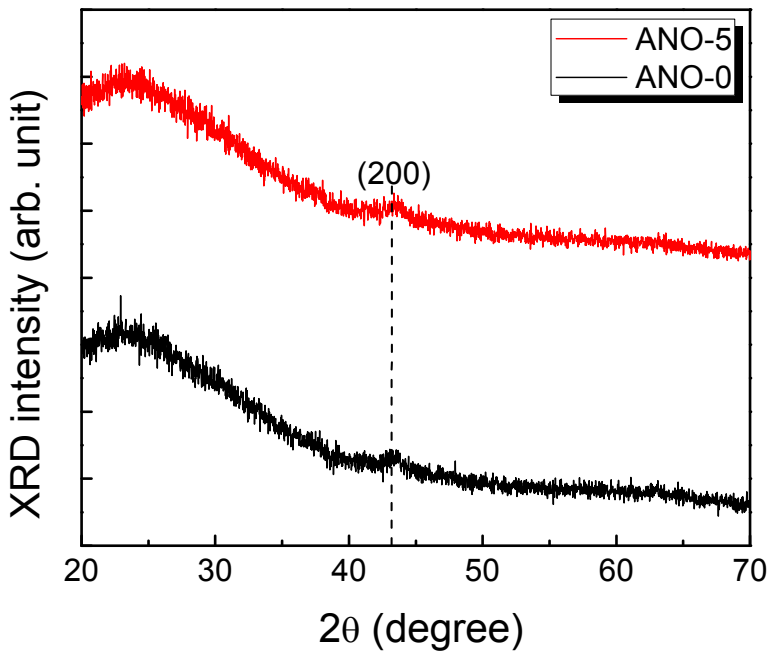

Figure S2 XRD patterns of the ANO-0 and ANO-5 films prepared by spin-coating precursors 6 times on glasses.

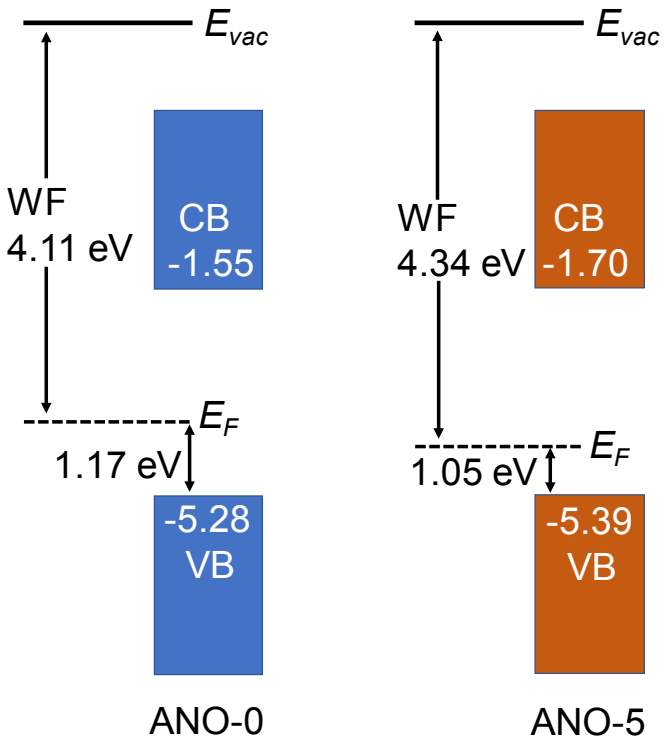

Figure S3 Schematic energy level diagrams for the ANO-0 and ANO-5 films based on the parameters derived from the UPS spectra and optical absorption measurements

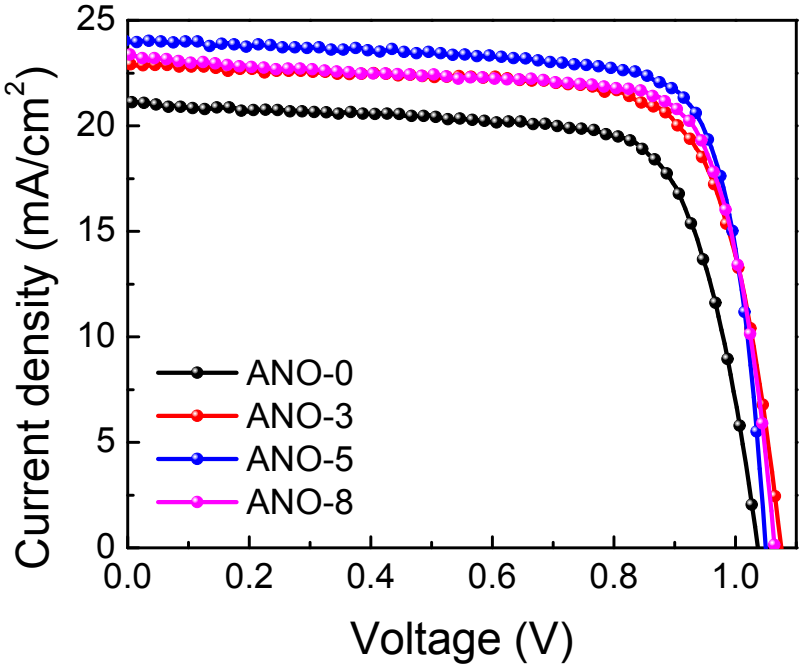

Figure S4. J-V characteristics of the PSCs with ANO-0, ANO-3, ANO-5, and ANO-8 HTLs measured under standard test conditions (AM1.5G, 100 mW/cm^2).

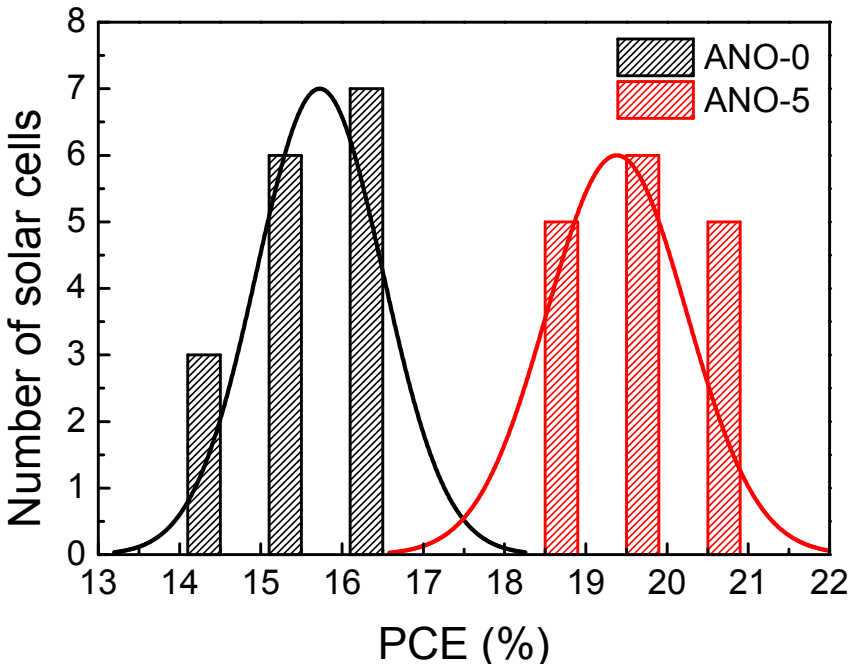

Figure S5. PCE distribution of 16 devices with ANO-0 and ANO-5 HTLs.

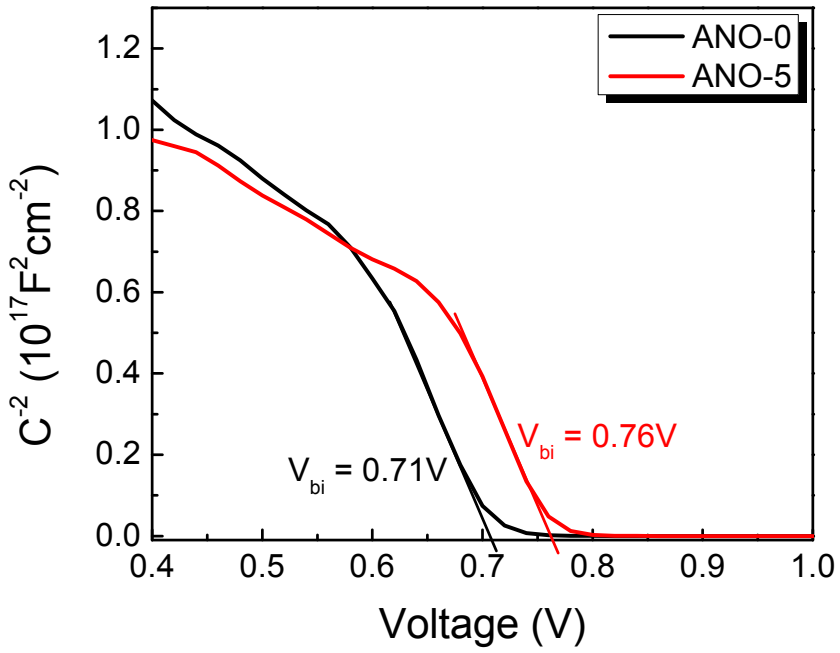

Figure S6. Mott−Schottky plots of capacitance−voltage measurements of the PSCs based on the ANO-0 and ANO-5 HTLs.

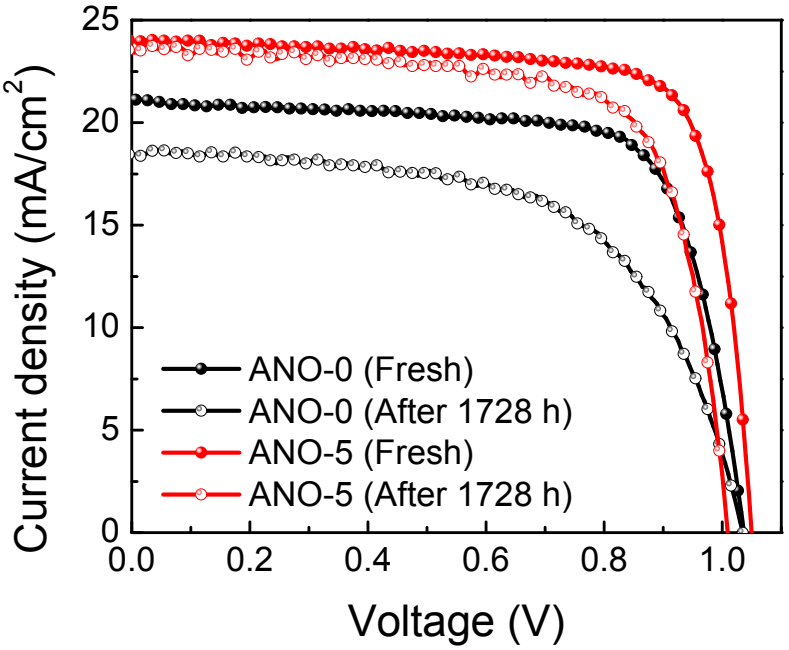

Figure S7. J-V curves of the unencapsulated ANO-0 and ANO-5 HTL-based PSCs stored in a nitrogen-filled glove box for over 1728 h (72 d).

Table S1. Photovoltaic parameters of the PSCs with ANO-0, ANO-3, ANO-5, and ANO-8 HTLs measured under standard test conditions (AM1.5G, 100 mW/cm^2).

Sample	PCE (%)	V_{oc} (V)	J_{sc} (mA/cm^2)	FF (%)
ANO-0	16.56	1.03	21.00	75.96
ANO-3	18.75	1.07	23.66	73.76
ANO-5	20.84	1.06	24.34	81.31
ANO-8	19.34	1.06	23.76	76.81

Table S2. Average performance of 16 PSCs with ANO-0 and ANO-5 HTLs.

Samples		PCE (%)	V_{oc} (V)	J_{sc} (mA/cm^2)	FF (%)
ANO-0	Average	15.72±0.8	1.02±0.05	20.24±0.72	74.44±4.58
	Best	16.56	1.03	21.00	75.96
ANO-5	Average	19.37±1.27	1.04±0.02	23.82±0.35	78.02±2.25
	Best	20.84	1.06	24.34	81.31

Table S3. Summary of high-performance $MAPbI_3$ PSCs with several metal-doped NiO_x HTLs reported in the literature and their corresponding device structures.

Device structure	J_{sc} (mA/cm^2)	V_{oc} (V)	FF (%)	PCE (%)	Method/ Temperature	Ref.
FTO/NiO_x/$MAPbI_3$/PCBM/Ag	17.9	1.09	73.8	14.4	Spin-coating /550 °C	[1]
FTO/NiO/$MAPbI_3$/PCBM/Ag	14.1	1.08	58.0	8.7	Spin-coating /550 °C	[2]
FTO/Cu:NiO_x/$MAPbI_3$/PCBM/Ag	18.8	1.11	72.0	15.4	Spin-coating /550 °C	[2]
FTO/NiMgLiO/$MAPbI_3$/PCBM/Ti(Nb)O_x/Ag	20.6	1.07	74.8	16.2	Spray pyrolysis /500 °C	[3]
FTO/NiMgLiO/$MAPbI_3$/PCBM/Ti(Nb)O_x/Ag	22.8	1.12	77.2	19.6	Spray pyrolysis /500 °C	[4]
FTO/NiMgLiO/$MAPbI_3$/PCBM/Ti(Nb)O_x/Ag	22.6	1.12	75.7	19.2	Spray pyrolysis /500 °C	[4]
FTO/Cs:NiO_x/ $MAPbI_3$/PCBM/BCP/Au	21.4	1.03	78.0	17.2	Spin-coating /500 °C	[5]
ITO/NiO_x(NP)/$MAPbI_3$/PCBM/BCP/Ag	20.6	1.03	74.7	15.9	NP ink/RT	[6]

ITO/NiO_x(NP)/$MAPbI_3$/PCBM/Rhodamine/Ag	21.2	1.04	75.0	16.6	NPs/RT	[7]
ITO/NiO_x/$MAPbI_3$/PCBM/ZnO/Ag	21.0	1.01	76.0	16.1	Spin-coating /300 °C	[8]
FTO/NiO_x/$MAPbI_3$/PCBM/Ag	20.5	0.99	77.5	15.7	Spin-coating /350 °C	[9]
ITO/NiO_x/$MAPbI_3$/PCBM/LiF/Al	20.2	1.06	81.3	17.3	PLD/200 °C	[10]
ITO/NiO_x/$MAPbI_3$/PCBM/Ag	21.8	1.04	72.0	16.4	ALD/300 °C	[11]
ITO/Cu:NiO_x(NP)/$MAPbI_3$/Bis-60/C60/Ag	22.03	1.05	76.0	17.7	Combustion NPs/300 °C	[12]
ITO/Cu:NiO_x/$MAPbI_3$/PCBM:C60(1:1)/Bis-C60/Ag	20.1	1.05	73.0	15.4	Spin-coating /300 °C	[13]
FTO/K:NiO/$MAPbI_3$/PCBM/C60/BCP/Ag	22.77	1.01	78.1	18.0	Spin-coating /400 °C	[14]
ITO/Co:NiO_x/$MAPbI_3$/PCBM/Ag	22.3	1.05	79.0	18.6	Spin-coating /400 °C	[15]
ITO/Fe:NiO_x/ $MAPbI_3$/PCBM/BCP/Ag	19.1	1.08	84.4	17.4	NPs/RT	[16]
FTO/Y:NiO/ $MAPbI_3$/PCBMAu	23.82	1.00	68.0	16.3	Spin-coating /500 °C	[17]
ITO/Ag:NiO_x/ $MAPbI_3$/PCBM/BCP/Ag	20.8	1.06	78.0	17.2	Spin-coating /300 °C	[18]
ITO/Cu:NiO/$MAPbI_3$/C_{60}/BCP/Ag	22.23	1.12	80.90	20.15	NP/RT	[19]
FTO/Zn:NiO_x/$MAPbI_3$/PCBM/BCP/Ag	22.80	1.10	78.00	19.60	Spin-coating /400 °C	[20]
FTO/Cs:NiO_x/$MAPbI_3$/PCBM/ZrAcac/Ag	21.77	1.12	78.00	19.35	Spin-coating /275 °C	[21]
ITO/LiAg:NiO_x/$MAPbI_3$/PCBM/BCP/Ag	21.29	1.13	74.80	19.24	Spin-coating /300 °C	[22]
ITO/NiO_x/$MAPbI_3$/PCBM/AM-TiO_x/Ag	**21.0**	**1.03**	**75.9**	**16.56**	**Spin-coating /300 °C**	**This work**
ITO/Al:NiO_x/$MAPbI_3$/PCBM/AM-TiO_x/Ag	**24.34**	**1.06**	**81.3**	**20.84**	**Spin-coating /300 °C**	**This work**

Table S4. Performance parameters of unencapsulated ANO-0 and ANO-5 HTL-based PSCs stored in a nitrogen-filled glove box for over 1728 h (72 days).

Samples	PCE (%)	V_{oc} (V)	J_{sc} (mA/cm^2)	FF (%)	Stability (%)
ANO-0 (fresh)	16.56	1.03	21.00	75.96	75.5
ANO-0 (1728 h)	12.51	1.03	18.95	64.08	
ANO-5 (fresh)	20.84	1.06	24.34	81.31	84.3
ANO-5 (1728 h)	17.57	1.01	23.65	73.31	

References:

1. Yin, X.; Que, M.; Xing, Y.; Que, W. High Efficiency Hysteresis-Less Inverted Planar Heterojunction Perovskite Solar Cells with a Solution-Derived NiO*x* Hole Contact Layer. *J. Mater. Chem. A* **2015**, 3, 24495-24503.
2. Kim, J. H.; Liang, P. W.; Williams, S. T.; Cho, N.; Chueh, C. C.; Glaz, M. S.; Ginger, D. S.; Jen, A. K. High-Performance and Environmentally Stable Planar Heterojunction Perovskite Solar Cells Based on a Solution-Processed Copper-Doped Nickel Oxide Hole-Transporting Layer. *Adv. Mater.* **2015**, 27, 695-701.
3. Chen, W.; Wu, Y.; Yue, Y.; Liu, J.; Zhang, W.; Yang, X.; Chen, H.; Bi, E.; Ashraful, I.; Grätzel, M. Efficient and Stable Large-Area Perovskite Solar Cells with Inorganic Charge Extraction Layers. *Science* **2015**, 350, 944-948.

4. Wu, Y.; Xie, F.; Chen, H.; Yang, X.; Su, H.; Cai, M.; Zhou, Z.; Noda, T.; Han, L. Thermally Stable $MAPbI_3$ Perovskite Solar Cells with Efficiency of 19.19% and Area over 1 cm^2 Achieved by Additive Engineering. *Adv. Mater.* **2017**, 29, 1701073.

5. Kim, H-S; Seo, J-Y; Xie, H; Lira-Cantu, M; Zakeeruddin, S. M.; Gratzel, M; Hagfeldt, A. Effect of Cs-Incorporated NiOx on the Performance of Perovskite Solar Cells. *ACS Omega* **2017**, 2, 9074−9079.

6. Cao, J.; Yu, H.; Zhou, S.; Qin, M.; Lau, T.-K.; Lu, X.; Zhao, N.; Wong, C.-P.Low-Temperature Solution-Processed NiO*x* Films for Air-Stable Perovskite Solar Cells. *J. Mater. Chem. A* **2017**, 5, 11071–11077.

7. Ciro, J.; Ramirez, D.; Mejia Escobar, M. A.; Montoya, J. F.; Mesa, S.; Betancur, R.; Jaramillo, F. Self-Functionalization Behind a Solution-Processed NiO*x* Film Used As Hole Transporting Layer for Efficient Perovskite Solar Cells. *ACS Appl. Mater. Inter.* **2017**, 9, 12348-12354.

8. You, J.; Meng, L.; Song, T. B.; Guo, T. F.; Yang, Y. M.; Chang, W. H.; Hong, Z.; Chen, H.; Zhou, H.; Chen, Q.; Liu, Y.; De Marco, N.; Yang, Y. Improved Air Stability of Perovskite Solar Cells via Solution-Processed Metal Oxide Transport Layers. *Nat. Nanotechnol.* **2016**, 11, 75-81.

9. Yin, X.; Yao, Z.; Luo, Q.; Dai, X.; Zhou, Y.; Zhang, Y.; Zhou, Y.; Luo, S.; Li, J.; Wang, N.; Lin, H. High Efficiency Inverted Planar Perovskite Solar Cells with Solution-Processed NiOx Hole Contact. *ACS Appl. Mater. Inter.* **2017**, 9, 2439-2448.

10. Park, J. H.; Seo, J.; Park, S.; Shin, S. S.; Kim, Y. C.; Jeon, N. J.; Shin, H. W.; Ahn,T. K.; Noh, J. H.; Yoon, S. C.; Hwang, C. S.; Seok, S. I. Efficient $CH_3NH_3PbI_3$ Perovskite Solar Cells Employing Nanostructured p-Type NiO Electrode Formed by a Pulsed Laser Deposition. *Adv. Mater.* **2015**, 27, 4013-4019.

11. Seo, S.; Park, I. J.; Kim, M.; Lee, S.; Bae, C.; Jung, H. S.; Park, N. G.; Kim, J. Y.; Shin, H. An Ultra-Thin, Un-Doped NiO Hole Transporting Layer of Highly Efficient (16.4%) Organic-Inorganic Hybrid Perovskite Solar Cells. *Nanoscale* **2016**, 8, 11403-11412.
12. Jung, J. W.; Chueh, C. C.; Jen, A. K. A Low-Temperature, Solution-Processable, Cu-Doped Nickel Oxide Hole-Transporting Layer via the Combustion Method for High-Performance Thin-Film Perovskite Solar Cells. *Adv. Mater.* **2015**, 27, 7874-80.
13. Yang, Z.; Chueh, C. C.; Liang, P. W.; Crump, M.; Lin, F.; Zhu, Z.; Jen, A. K. Y. Effects of Formamidinium and Bromide Ion Substitution in Methylammonium Lead Triiodide toward High-Performance Perovskite Solar Cells. *Nano Energy* **2016**, 22, 328-337.
14. Yin, X. W.; Han, J. H.; Zhou, Y.; Gu, Y. C.; Tai, M. Q.; Nan, H.; Zhou, Y. Y.; Li, J. B.; Lin, H. Critical roles of potassium in charge-carrier balance and diffusion induced defect passivation for efficient inverted perovskite solar cells. *J. Mater. Chem. A* **2019**, *7*, 5666– 5676.
15. Xie, Y.; Lu, K.; Duan, J.; Jiang, Y.; Hu, L.; Liu, T.; Zhou, Y.; Hu, B. Enhancing Photovoltaic Performance of Inverted Planar Perovskite Solar Cells by Cobalt-Doped Nickel Oxide Hole Transport Layer. *ACS Appl. Mater. Interfaces* **2018**, 10, 14153−14159.
16. Chandrasekhar, P.S.; Seo, Y-H.; Noh, Y-J.; Na, S-I. Room Temperature Solution-Processed Fe Doped NiOx as a Novel Hole Transport Layer for High Efficient Perovskite Solar Cells. *Appl. Surf. Sci.* **2019**, 481, 588-596.
17. Hu, Z.; Chen, D.; Yang, P.; Yang, L.; Qin, L.; Huang, Y.; Zhao, X. Sol-gel-processed Yttrium-Doped NiO as Hole Transport Layer in Inverted Perovskite Solar Cells for Enhanced Performance. *Appl. Surf. Sci.* **2018**, 441, 258-264.
18. Zheng, J.; Hu, L.; Yun, J. S.; Zhang, M.; Lau, C. F. J.; Bing, J.; Deng, X.; Ma, Q.; Cho, Y.; Fu, W.; Chen, C.; Green, M. A.; Huang, S.; Ho-Baillie, A. W. Y. Solution-Processed Silver-

Doped NiO_x as Hole Transporting Layer for High-Efficiency Inverted Perovskite Solar Cells. : *ACS Appl. Energy Mater.* **2018,** *1* (2), 561-570.

19. Chen, W.; Wu, Y. Wu.; Fan, J.; Djurišić,A. B.; Liu, F.; Tam, H. W.; Ng, A.; Surya, C.; Chan, W. K.; Wang, D.; He, Z.-B. Understanding the Doping Effect on NiO: Toward High-Performance Inverted Perovskite Solar Cells. *Adv. Energy Mater*. **2018**, 8, 1703519.
20. Wan, X.; Jiang, Y.; Qui, Z.;Zhang, H.; Zhu, X.; Sikandar, I.; Liu, X.; Chen, X.; Cao, B. Zinc as a New Dopant for NiOx-Based Planar Perovskite Solar Cells with stable efficiency near 20%. *ACS Appl. Energy Mater*. **2018**, 1, 3947-3954.
21. Chen, W.; Liu, F.-Z.; Feng, X.-Y.; Djurišić, A. B.; Chan, W. K.; He, Z.-B. Cesium Doped NiO_x as an Efficient Hole Extraction Layer for Inverted Planar Perovskite Solar Cells. *Adv. Energy Mater*. **2017**, 7, 1700722.
22. Xia, X.; Jiang, Y.; Wan, Q.; Wang, X.; Wang, L.; Li, F., Lithium and Silver Co-Doped Nickel Oxide Hole-Transporting Layer Boosting the Efficiency and Stability of Inverted Planar Perovskite Solar Cells. *ACS Applied Materials & Interfaces* **2018,** 10, (51), 44501-44510.